Kinetics of Cardiac Glycoside Binding to Sodium, Potassium Adenosine Triphosphatase Studied with a Fluorescent Derivative of Ouabain†

Edward G. Moczydlowski and P. A. George Fortes*

ABSTRACT: We have studied the kinetics of the interaction of a fluorescent derivative of ouabain, anthroylouabain (AO) [Fortes, P. A. G. (1977) *Biochemistry 16*, 531], with purified Na,K-ATPase preparations from rabbit kidney and eel electroplax. The dependence of the rate of AO binding on pH and the concentration of ATP, P_i, Mg^{2+}, Mn^{2+}, and Co^{2+} was also studied. AO binding kinetics is first order for both enzymes under all ligand conditions when [AO] ≫ [ATPase], except for the eel enzyme with Mg + P_i which appears to show two components that differ about fourfold in rate. However, in the presence of 2 mM K^+ or when [ATPase] ≫ [AO], the eel enzyme also shows first-order kinetics with Mg^{2+} + P_i, suggesting the existence of two slowly interconvertible conformations with different kinetic properties. Dissociation constants for AO derived from kinetic measurements agree with those derived from equilibrium binding. The eel Na,K-ATPase has a faster AO association rate and a significantly slower AO dissociation rate than the rabbit Na,K-ATPase, resulting in a 10-fold higher affinity in the former. Both enzymes show faster AO binding at pH 6.2 than at pH 7.5 with Mg^{2+} + P_i. The dependence of AO binding rate on ATP, P_i, and Mn^{2+} concentration is hyperbolic, but Mg^{2+} and Co^{2+} give sigmoid curves with Hill coefficients of 1.3–1.5. The apparent affinity for divalent metals derived from AO binding kinetics decreases with decreasing ionic radius: $Mn^{2+} > Co^{2+} > Mg^{2+}$ for both eel and rabbit enzymes. Co^{2+} and Mn^{2+} support the same AO binding rates as Mg^{2+}, except in the rabbit enzyme where the maximal rate observed in the presence of Mn^{2+} is only one-fifth of that with Mg^{2+} or Co^{2+}.

Active transport of sodium and potassium by the Na–K pump is thought to be effected by a series of conformational changes of the Na,K-ATPase[1] during ATP hydrolysis (Post, 1977; Karlish et al., 1978b).

Cardiac glycosides are specific inhibitors of the Na–K pump (Glynn, 1964). The affinity of the receptor and the kinetics of cardiac glycoside association and dissociation are modulated by the various ligands through their effect on the phosphoenzyme, which is the form that binds cardiac glycosides (Schwartz et al., 1968, 1975; Sen et al., 1969; Albers et al., 1968). Thus, the binding of cardiac glycosides is a useful parameter to study the mechanism of the Na–K pump. Most studies of cardiac glycoside interaction with Na,K-ATPase have been done by measuring binding of radioactive glycosides (Erdmann & Schoner, 1973a,b; Wallic & Schwartz, 1974; Hansen & Skou, 1973; Choi & Akera, 1977, 1978) or indirectly by measuring inhibition of enzyme activity (Kyte, 1972; Yoda et al., 1973; Yoda, 1974). As an alternative approach, we have synthesized a fluorescent derivative of ouabain, anthroylouabain (AO), that resembles ouabain in its specificity, inhibitory action, and ligand requirements for interaction with the Na,K-ATPase (Fortes, 1977). AO binding to the Na,K-ATPase results in a large fluorescence enhancement. This allows direct and continuous spectroscopic monitoring of the glycoside–Na,K-ATPase interaction even at low enzyme concentrations (10^{-8}–10^{-7} M) and circumvents the need for washing or processing samples in any way.

In this paper we report a detailed kinetic study of the interaction of AO with purified Na,K-ATPases from rabbit kidney and eel electroplax as a function of ATP, P_i, and divalent cation concentrations. We show that AO and ouabain have similar kinetic parameters, and the results obtained with AO fluorescence measurements are similar to those reported using other methods. We present quantitative differences between the eel and rabbit enzymes and ligand affinity constants derived from the kinetic measurements.

Materials and Methods

Enzyme Preparations. Eel electroplax Na,K-ATPase was purified according to the procedure of Perrone et al. (1975) as described elsewhere (Jesaitis & Fortes, 1980). Live electric eels were obtained from World Wide Scientific Animals (Ardsley, NY). Polyacrylamide gel electrophoresis in sodium dodecyl sulfate showed only the two polypeptides characteristic of the pure enzyme. The specific activity of the eel enzyme preparations ranged from 22 to 27 μmol of ATP per min per mg assayed at 37 °C with 3 mM Na_3ATP, 3 mM $MgCl_2$, 100 mM NaCl, 20 mM KCl, and 30 mM histidine, pH 7.5. Under these conditions, ATP hydrolysis was linear during the time of the assay (5 min). Inorganic phosphate was measured according to Taussky & Shorr (1953). The trinitrophenyl-ATP (Fortes & Moczydlowski, 1977) and AO binding capacity of the eel enzyme ranged from 3.7 to 4.3 nmol/mg as determined by fluorescence titrations carried out as described previously (Fortes, 1977). Rabbit kidney Na,K-ATPase was purified by the method of Jorgensen (1974a) as previously described (Fortes, 1977). Gel electrophoresis showed the two polypeptides characteristic of the ATPase plus minor contaminating bands. The specific activity of the rabbit enzyme ranged from 15 to 23 μmol of ATP per min per mg, and the AO binding capacity was 2 to 3 nmol/mg. Ouabain-insensitive activity was less than 1% in the eel and rabbit preparations. Purified enzyme was suspended at ~5–10 mg/mL in 1 mM

† From the Department of Biology, C-016, University of California, San Diego, La Jolla, California 92093. *Received March 20, 1979.* This work was supported by Grant 74-1072 from the American Heart Association and Grants HL-20262 and RR-08135 from the National Institutes of Health. E.G.M. was supported by U.S. Public Health Service Predoctoral Training Grant GM 07313-5T32.

[1] Abbreviations used: AO, anthroylouabain; Hepes, 4-(2-hydroxyethyl)-1-piperazineethanesulfonic acid; Pipes, 1,4-piperazinediethanesulfonic acid; Tris, tris(hydroxymethyl)aminomethane; EDTA, ethylenediaminetetraacetic acid; CDTA, *trans*-1,2-diaminocyclohexanetetraacetic acid; P_i, inorganic phosphate; Na,K-ATPase, sodium, potassium adenosine triphosphatase.

0006-2960/80/0419-0969$01.00/0

Tris-HCl and 0.1 mM CDTA, pH 7.0, frozen in liquid N_2, and stored in small aliquots at −80 °C. Vials of enzyme were thawed at 0 °C just before use and were kept on ice.

Fluorescence Measurements. Binding reactions were carried out in 1 × 1 cm, quartz fluorescence cuvettes at a total volume of 1.6–2.0 mL in a cuvette holder kept at constant temperature by means of a thermostated circulating water bath. The contents of the cuvette were continuously stirred by means of a Teflon-coated spin bar. A Hitachi Perkin-Elmer MPF-4 spectrofluorometer was used in the ratio mode, and AO fluorescence was excited at 370 nm through a CS 7-51 Corning filter. The emission monochromator was removed from the path to the photomultiplier by setting the wavelength to zero, and a Corning CS 3-71 cutoff filter was placed on the emission side of the cuvette. This filter absorbs light below 470 nm. The excitation and emission slits were set at 10 nm. This arrangement provided maximum sensitivity and a low noise signal. In some experiments the emission monochromator was set at 485 nm.

Binding was usually measured at low enzyme concentration with excess AO to achieve pseudo-first-order conditions, and most of the fluorescence signal resulted from the unbound AO in solution. For magnification of the portion of the signal due to binding, the amplifier was set at high gain and the signal was brought back on scale by means of the zero supression backoff voltage. Under these conditions the maximum binding signal spanned most of the 23-cm chart paper when 30–50 μg of purified rabbit or eel enzyme was used and was actually equivalent to 10–20% of the total fluorescence.

Binding Assays. The buffers used in these experiments were Hepes–Tris, pH 7.5, or Pipes–Tris, pH 6.2, which are reported to have negligible affinity for divalent cations (Good et al., 1966). Histidine buffers could not be used because histidine forms a highly colored complex with Co^{2+}. Most of the experiments were done at pH 6.2 because Mn^{2+} and Co^{2+} form precipitates with P_i at pH 7.5 and the formation of these precipitates was found to be much slower at pH 6.2. For experiments at low ATP concentration, the ATP concentration was maintained constant by means of a creatine phosphate plus creatine kinase regenerating system.

For the experiments in Figure 1, a small fluorescence increase is observed when EDTA is added, which is an artifact that is also observed in the absence of enzyme, indicating that it is due to a small effect on the free AO. There is a slight decrease in the pH of the medium under the conditions of this experiment that occurs when H^+ is released from EDTA after a metal ion is complexed. This pH decrease amounts to 0.2 pH unit at 5 mM divalent metal. However, the pH change does not seem to be responsible for the artifact since AO fluorescence in H_2O is insensitive to changes in pH from 5.5 to 8.5. The artifact is sensitive to ionic strength since it was eliminated at twice the buffer concentration. It is not due to fluorescent contaminants in the EDTA or metal ion solutions, since addition of either of these alone does not cause a fluorescence increase. It is probable that this artifact may be due to a weak interaction between AO and EDTA–Me^{2+} complexes in solution.

For the kinetic experiments in which the pseudo-first-order association rate constant was measured, straight lines were drawn through the data plotted on a semilog plot. In the case of the kinetics of the eel enzyme in the presence of Mg^{2+} and P_i, the data could be fitted by a sum of two exponentials according to the equation $1 - (\Delta F/\Delta F_\infty) = Ae^{-k_1 t} + Be^{-k_2 t}$, where A is the fraction following the fast rate constant, k_1, and B is the fraction following the slow rate constant, k_2 ($A + B = 1$). k_2 and B were obtained from the slope and intercept of a straight line drawn through the data at long times. Subtraction of this line from the whole time course gave a straight line with slope = $-k_1$ and intercept = A. Initial rates of binding were measured by drawing a tangent to the initial part of the binding trace, and the slope of this line was taken as the velocity expressed in arbitrary fluorescence units per unit time. In cases where double-reciprocal plots of velocity or rate constants vs. concentration were linear, the $K_{0.5}$ and maximal rate given by the intercepts were determined by a linear regression of the data. In cases where the double-reciprocal plots exhibited curvature, the $K_{0.5}$ was determined from a linear regression of the Hill plot in which the value for the maximum rate was obtained from the apparent ordinate intercept of the double-reciprocal plot.

Duplicate runs gave superimposable traces, and the kinetic parameters derived from similar experiments done on different days and/or with different enzyme preparations varied less than 10%.

AO binding assays in the presence of $CoSO_4$ were complicated by quenching of the receptor-specific AO fluorescence (Moczydlowski & Fortes, 1977a,b). Since addition of EDTA reverses Co^{2+} quenching, the equivalent unquenched fluorescence of AO bound to the enzyme was measured at each cobalt concentration by adding EDTA after equilibrium was reached. The fluorescence values during the binding reaction were corrected for quenching by dividing the observed rate by the fractional quenching (i.e., by the ratio of fluorescence before and after EDTA addition). This effect prevented examination of AO binding to the rabbit enzyme at high Co^{2+} concentrations because the quenching was greater than 80% and required large corrections. For the experiments with Co^{2+} in this paper (Figure 7), the fluorescence of bound AO was quenched a maximum of 20% at the highest Co^{2+} concentration used. Thus, the observed initial velocity was divided by 0.8 or multiplied by a correction factor of 1.25 in the worst case. In the range of Co^{2+} concentrations used in these experiments, corrections of the initial rate of binding due to the filter effect caused by absorption by Co^{2+} in the region of AO fluorescence were less than 2 to 3%.

Materials. The buffers, ATP, and phosphate solutions were treated batchwise with Chelex 100 metal chelating resin in the acid form in order to remove contaminating metal ions. Chelex 100 (50–100 mesh) resin was obtained from Bio-Rad Laboratories and was washed according to Williard et al. (1969). Na_2ATP was converted to the Tris salt by treatment with Dowex-50W in the acid form; the ATP was subsequently treated with Chelex and neutralized with Tris base, and the ATP concentration was determined by measuring the absorbance at 259 nm using the molar extinction coefficient of 15.4×10^3. Inorganic phosphate solutions were prepared from phosphoric acid neutralized with Tris base. AO was synthesized and purified as previously described (Fortes, 1977). The disodium salt of ATP, the disodium salt of creatine phosphate, and creatine kinase were obtained from Boehringer Mannheim. $MgCl_2$ and $MnCl_2$ were obtained from Baker, and $CoSO_4$ was obtained from Gallard Schlesinger. All other chemicals were reagent grade.

Results

Kinetics of AO Interaction with the Na,K-ATPase. Typical chart traces of fluorescence measurements of AO binding to eel and rabbit Na,K-ATPase are shown in Figure 1. In these experiments, Mg^{2+} or Mn^{2+} was first added to a cuvette containing AO and enzyme and the fluorescence was essentially constant over the next 20 s except for a small initial

Table I: Kinetic Constants for AO Binding[a]

enzyme source	ligands	pH	k_p ($\times 10^{-2}$ s^{-1})	k_{off} ($\times 10^{-4}$ s^{-1})	k_{on} ($\times 10^{3}$ M^{-1} s^{-1})	$k_D = k_{off}/k_{on}$ ($\times 10^{-8}$ M)
rabbit	Mg + P_i	6.2	1.9	4.9	5.8	8.4
rabbit	Mg + P_i	7.5	0.95	3.0	2.9	10
rabbit	MgATP + Na	6.2	1.2	11.0	3.6	31
rabbit	MgATP + Na	7.5	0.62	3.7	1.9	19
eel	Mg + P_i	6.2	2.4, 9.6[b] (7.1)[c]	0.84	7.3, 29.1[b] (21.5)[c]	0.29, 1.15[b] (0.39)[c]
eel	Mg + P_i	7.5	0.37, 1.8[b] (1.5)[c]		1.2, 6[b] (5)[c]	
eel	MgATP + Na	6.2	4.5	1.7	14	1.2
eel	MgATP + Na	7.5	5.2		16	

[a] Conditions are as in Figures 2 and 4. At pH 7.5 the buffer was 45 mM Tris-HCl. [b] The two values listed correspond to the slow and fast rate constants k_1 and k_2. [c] The numbers in parentheses are the weighted-average rate constants obtained as $k_{av} = Ak_1 + Bk_2$.

dilution artifact. When P_i was subsequently added, the fluorescence increased to a new equilibrium level. This increase corresponds to the binding of AO to the cardiac glycoside receptor and is due to an increase in the quantum yield of the bound vs. free AO (Fortes, 1977). If excess ouabain (0.1–1 mM) is included in the cuvette, the fluorescence increase is not observed, indicating that it represents a specific interaction. On a longer time scale than that of Figure 1, slow AO binding is observed in the presence of Mg^{2+} alone as reported previously (Fortes, 1977). Mn^{2+} can substitute for Mg^{2+}, resulting in an identical binding rate with the eel enzyme (Figure 1A). The rabbit enzyme, however, exhibits faster binding kinetics with Mg^{2+} than Mn^{2+}, although both ligands are present at near saturating concentrations (parts B and C of Figure 1). In addition, the total change in fluorescence with Mn^{2+} was ~24% less than that with Mg^{2+} under these experimental conditions. This suggests that less AO was bound, probably due to a lower AO binding affinity in the presence of Mn^{2+} (see below).

A survey of divalent cations showed that Mg^{2+}, Mn^{2+}, and Co^{2+} promote AO binding. Ca^{2+} and Ni^{2+} appear to promote AO binding only at a very slow rate, while Cu^{2+} and Zn^{2+} inhibit AO binding or induce AO dissociation at micromolar concentrations.

Figure 1 also shows that addition of sufficient EDTA to chelate all the free divalent cations causes a slow fluorescence decrease that reflects AO dissociation, similar to that observed with addition of excess ouabain (Fortes, 1977). The small fluorescence increase seen immediately after EDTA addition appears to be an artifact, since it is also observed in the absence of enzyme (see Materials and Methods).

The kinetics of AO binding may be treated as a bimolecular reaction between AO and the high-affinity form of the receptor:

$$R + AO \underset{k_{off}}{\overset{k_{on}}{\rightleftharpoons}} R{\cdot}AO$$

Under pseudo-first-order conditions, when one of the reactants is in large excess over the other, the integrated rate expression for the approach to equilibrium is

$$\ln\left(1 - \frac{[R{\cdot}AO]_t}{[R{\cdot}AO]_\infty}\right) = -(k_p + k_{off})t \qquad (1)$$

where $[R{\cdot}AO]_t$ and $[R{\cdot}AO]_\infty$ are the concentrations of complexed receptor at time t and equilibrium, respectively, and $k_p = k_{on}[AO]$ or $k_p = k_{on}[R]$. Since the fluorescence enhancement is a measure of the concentration of the R·AO complex, eq 1 may also be expressed in terms of ΔF and ΔF_∞, which are the respective fluorescence changes at time t and equilibrium, relative to the initial fluorescence.

The kinetics of AO association to rabbit and eel enzymes in the presence of either Mg + P_i or MgATP + Na were studied at pH 6.2 and 7.5. The results of typical experiments, plotted according to eq 1, are shown in Figure 2, and the derived rate constants are shown in Table I. When AO concentration is in excess over the rabbit enzyme, the plots are linear for at least 80–95% of the equilibrium value regardless of the pH or whether binding is promoted by MgATP + Na or Mg + P_i. However, a small deviation from linearity is apparent after more than 90% of the equilibrium value is reached (curve C in Figure 2). The rate of this slower component is about half of that of the main component. It is not

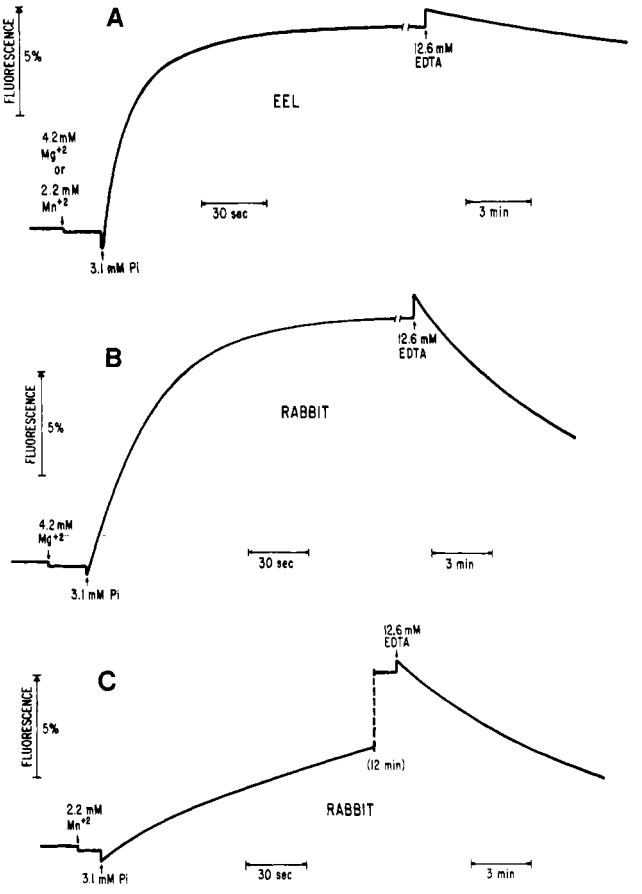

FIGURE 1: Time course of AO binding and dissociation. The cuvettes had 2.6 μM AO, 46 mM Pipes–Tris (pH 6.2), and 26 μg/mL eel (A) or 20 μg/mL rabbit (B and C) Na,K-ATPase. Temperature was 25 °C. At the arrows $MgCl_2$, $MnCl_2$, Tris–P_i, or EDTA was added at the indicated final concentrations. The small fluorescence decreases with the additions are due to dilution. The fluorescence increase with EDTA is also seen with no enzyme (see Materials and Methods). In (C) 12 min of the trace is omitted at the dotted line. Note that different time scales were used during the on and off reactions as indicated. The ordinate calibration is 5% of the total fluorescence. λ_{ex} = 370 nm. Emission was measured through a Corning CS 3-71 filter.

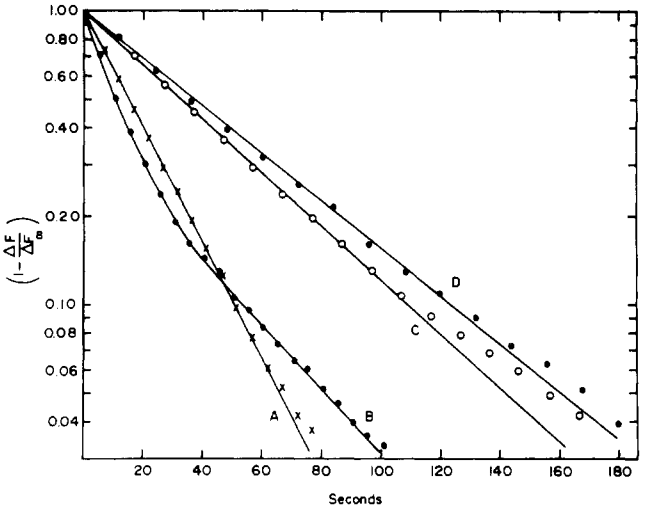

FIGURE 2: AO association kinetics. Curves A, B, and C are pseudo first order in AO, while curve D is pseudo first order in enzyme. AO binding was initiated by adding either ATP (A) or P_i (B–D), as in Figure 1. ΔF and ΔF_∞ are the changes in fluorescence at time t and at equilibrium, respectively. The cuvettes contained 45 mM Pipes–Tris (pH 6.2), 7.2 mM $MgCl_2$, and the following: (A) 3.3 μM AO, 82 μg/mL eel Na,K-ATPase, 24 mM NaCl, and 48 μM ATP; (B) 3.3 μM AO, 82 μg/mL eel Na,K-ATPase, and 4.8 mM phosphate–Tris; (C) 3.3 μM AO, 32 μg/mL rabbit Na,K-ATPase, and 4.8 mM phosphate–Tris; (D) 0.038 μM AO, 230 μg/mL eel Na, K-ATPase, and 5 mM phosphate–Tris. Temperature was 25 °C. The solid line drawn through curve B was calculated with the equation $1 - (\Delta F/\Delta F_\infty) = A \exp(-k_1 t) + B \exp(-k_2 t)$ as described under Materials and Methods.

clear whether this nonlinearity is significant since it is not always observed and similar deviations can be due to small errors in ΔF_∞. When AO is in excess over the eel enzyme, the plots are linear for binding promoted by MgATP + Na (Figure 2, curve A) but nonlinear in the presence of Mg + P_i (Figure 2, curve B). The same behavior was observed at pH 7.5, although the rates were slower (Table I). These results indicate that AO binding obeys pseudo-first-order kinetics, except for the eel enzyme in the presence of Mg + P_i. For the latter case the approach to equilibrium fits a sum of two exponentials with the faster component comprising 65 and 78% of the total binding at pH 6.2 and 7.5, respectively, and the remainder binding at an approximately fourfold slower rate.

If AO binding with Mg + P_i is measured with the eel enzyme concentration in large excess over the AO concentration, so that the reaction is pseudo first order in enzyme, the binding plots are linear (Figure 2, curve D). This behavior suggests that the nonlinear plots, such as curve B in Figure 2, reflect a kinetic heterogeneity in the enzyme since the faster binding species are selected by the conditions of curve D. The derived bimolecular rate constant, k_{on}, for the eel enzyme measured at high enzyme concentration is 2.0×10^4 M^{-1} s^{-1}. This value is close to the estimated k_{on} (2.9×10^4 M^{-1} s^{-1}) of the fast component measured at high AO concentration under similar ligand conditions. If 2.7 mM K^+ is included in the Mg + P_i medium, the kinetic plots for the eel enzyme under the conditions of curve B in Figure 2 are also linear, although with a 10-fold slower rate (Figure 3). In contrast, inclusion of 12 mM Na^+ slows AO binding but does not alter the curvature of the plots (Figure 3).

The slopes of the plots in Figure 2 give $k_p + k_{off}$. The dissociation rate constant k_{off} can be measured independently from the time course of the fluorescence decrease induced by adding ouabain at high concentration (0.1–1 mM) after AO binding equilibrium is reached (Fortes, 1977). The results of such experiments, done under the same conditions as the

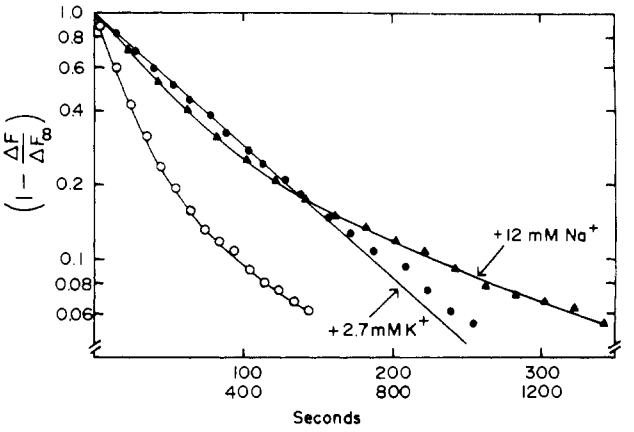

FIGURE 3: Effect of Na^+ and K^+ on the kinetics of Mg + P_i promoted AO binding to eel Na,K-ATPase. The cuvettes had 48 mM Pipes–Tris (pH 6.2), 4.4 mM P_i, 7.1 mM $MgCl_2$, 38 μg/mL eel Na, K-ATPase, 3.3 μM AO, and the indicated concentration of NaCl or KCl. Temperature = 25 °C. The lower time scale corresponds to the experiment in the presence of K (●) while the upper time scale corresponds to the experiments in the presence of Na (▲) and no alkali cations (○).

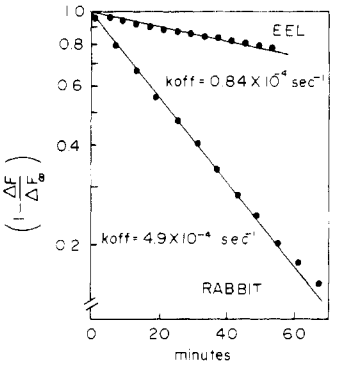

FIGURE 4: AO dissociation kinetics. The cuvettes had 45 mM Pipes–Tris (pH 6.2), 7.1 mM $MgCl_2$, 4.8 mM phosphate–Tris, 3.3 μM AO, and 32 μg/mL rabbit or 82 μg/mL eel Na,K-ATPase. Temperature 25 °C. AO dissociation was initiated by adding 0.29 mM ouabain at time 0. ΔF_∞ for the eel enzyme was estimated by assuming the F_∞ is equal to the fluorescence measured before AO binding was initiated.

binding reactions, are shown in Figure 4. The linear plots indicate that AO dissociation follows first-order kinetics for both rabbit and eel enzymes, with k_{off} about fivefold slower for the latter. The dissociation rate constant measured by adding excess EDTA, as in Figure 1, is similar within a factor of 2 to that measured by addition of excess ouabain. Thus, k_{off} is relatively unaffected by Mg^{2+} binding, indicating that the increase in affinity for AO caused by Mg^{2+} is primarily due to an increase in the association rate constant.

The slopes of the plots for the association reactions (Figure 2) are at least 11 times higher than those for the dissociation reactions (Figure 4), indicating that $k_p \gg k_{off}$ under these conditions. Therefore, the slopes of the association reactions at saturating ligand concentrations are essentially measures of the pseudo-first-order association rate constant k_p.

Table I summarizes the values of the kinetic constants under various ligand conditions and the derived equilibrium constants for AO binding. The eel enzyme has faster association and slower dissociation rates than the rabbit enzyme, resulting in higher AO affinity in the former. The dissociation constants derived from the kinetic measurements (Table I) are in agreement with those measured from equilibrium binding by fluorescence titration which give K_D = 10 and 100 nM for the

Scheme I

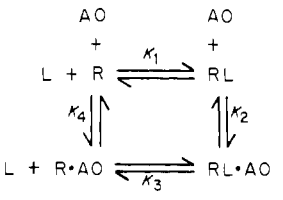

eel and rabbit enzymes, respectively.

The results in Table I also show that the rate constants are larger at pH 6.2 than at pH 7.5 in all cases except for the eel enzyme with MgATP + Na. A similar pH dependence of the ouabain binding rate in the presence of Mg + P_i has been reported by Yoda & Yoda (1978). This is in contrast with the Na,K-ATPase and phosphatase activities which exhibit a pH optimum around 7.5 (Dixon & Hokin, 1974; Gache et al., 1977; Schuurmans Stekhoven et al., 1976b).

Dependence of AO Binding Kinetics on Ligand Concentration. A simple model which describes the equilibria between AO, ligands, and the cardiac glycoside receptor is shown in Scheme I. In this scheme L represents one or a combination of the ligands that change the conformation of the receptor to the high-affinity form for cardiac glycosides (i.e., Mg + P_i or MgATP + Na), RL and R are the liganded and unliganded forms of the receptor, respectively, and K_1–K_4 are the corresponding ligand or AO dissociation constants ($K_i = k_{-i}/k_i$, i = 1–4). Scheme I is oversimplified when L = ATP or P_i since these ligands phosphorylate the enzyme. In this case reactions 1 and 3 include the formation and breakdown of both noncovalent and covalent intermediates (i.e., E·ATP, E·P_i, E~P, and E(~P)·ADP with and without divalent cation). Thus, K_1 and K_3 are not actual ATP or P_i dissociation constants but are overall apparent equilibrium constants for the binding and phosphorylation reactions.

When L = ATP in the presence of Mg^{2+} and Na^+, AO binds via reaction k_2; $k_4 \simeq 0$ since no binding is observed with Mg^{2+} + Na^+ in the absence of ATP (Fortes, 1977). Similarly, no binding occurs in the absence of divalent cations (Figure 1), indicating that $k_4 \simeq 0$. However, AO binds with Mg^{2+} alone in the absence of added phosphate (Fortes, 1977) so that AO binding in the presence of Mg + P_i may include both the P_i-dependent pathway k_1, k_2 and the P_i-independent pathway k_4. When L = P_i or ATP under phosphorylating conditions, AO dissocation may occur via both the k_{-2} and the k_{-3}, k_{-4} pathways, since the rate of enzyme dephosphorylation is faster than that of ouabain (Post et al., 1975) or cardiac aglycone (Yoda & Yoda, 1977) dissociation.

The quantum yield of the AO–ATPase complex appears to be the same regardless of the ligands present. The fluorescence spectra and intensities with saturating AO and ligand concentrations are identical in the presence of either Mg + P_i or MgATP + Na (Fortes, 1977). No significant fluorescence changes of bound AO are observed when Na, K, or EDTA are added, except the slow fluorescence decrease that reflects AO dissociation [Fortes (1977) and Figure 1]. Furthermore, the fluorescence lifetime of bound AO is not significantly different in the presence of various ligand combinations or immediately after the addition of EDTA (P. A. G. Fortes, unpublished experiments). Thus, it is reasonable to assume that the R·AO and RL·AO species are indistinguishable by fluorescence measurements and the observed fluorescence increase upon AO binding is a measure of [R·AO] + [RL·AO].

Assuming that the ligand interactions with the enzymes (reaction K_1) are in equilibrium compared with the AO association reactions K_2 and K_4, the initial rate of AO binding measured by changes in fluorescence can be described by

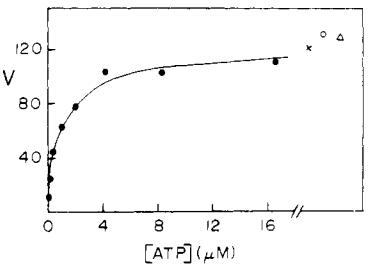

FIGURE 5: Effect of ATP on the initial rate of AO binding. The cuvettes had 47 mM Hepes–Tris (pH 7.5), 26 mM NaCl, 4.9 mM $MgCl_2$, 2.8 μM AO, 2.6 mM creatine phosphate, 0.12 mg/mL creatine kinase, 21 μg/mL eel Na,K-ATPase, and the indicated ATP concentrations. The symbols ×, ○, and △ correspond to 0.042, 0.41, and 0.83 mM ATP, respectively. Binding was initiated by addition of ATP. The ordinate shows the initial velocity in arbitrary fluorescence units per minute. The apparent K_m is 1 μM.

$$\frac{d([R\cdot AO] + [RL\cdot AO])}{dt} = V = k_4[AO][R] + k_2[AO][RL] \quad (2)$$

where k_2 and k_4 are the AO association rate constants for the liganded and unliganded receptor, respectively. After substituting for [RL] in terms of K_1 and [L], dividing by the total initial enzyme concentration $[E_T] = [R] + [RL]$, and rearranging, one obtains

$$V = \frac{k_4K_1[E_T][AO] + k_2[E_T][AO][L]}{K_1 + [L]} \quad (3)$$

When [L] = 0, AO binding will proceed along the ligand-independent path K_1 and the initial rate will equal $k_4[AO][E_T]$. If this rate, V_0, is subtracted from both sides of eq 3, the ligand-dependent velocity, $V - V_0$, is given by

$$V - V_0 = \frac{(k_2 - k_4)[E_T][AO][L]}{K_1 + [L]} \quad (4)$$

Equations 3 and 4 predict that plots of the initial velocity of AO binding vs. ligand concentration should be hyperbolic with a half-maximal velocity at a ligand concentration equal to the ligand dissociation constant K_1, i.e., equivalent to the Michaelis–Menten parameter K_m, if the rapid equilibrium assumption is valid. When the ligand is Mg^{2+}, AO does not bind in its absence. Therefore, $V_0 = 0$, $k_4 \ll k_2$, and $V_{max} = k_2[E_T][AO]$. However, for a ligand like P_i in the presence of saturating Mg^{2+}, AO binds slowly in the absence of P_i and k_4 is significant.

Effect of ATP. Figure 5 shows the initial velocity of AO binding to the eel Na,K-ATPase as a function of ATP concentration in the presence of Mg^{2+} and Na^+. A constant ATP concentration was maintained with creatine phosphate and creatine kinase. The AO binding rate increases with ATP concentration and is saturated around 10 μM ATP, with no further increases with up to 0.8 mM ATP. In the absence of added ATP a slow rate of AO binding was observed upon addition of both creatine phosphate and creatine kinase, but no binding occurred when either was added alone, indicating that some contaminating ADP (~0.08 μM) was present, probably associated with the Na,K-ATPase, since the enzyme is purified in the presence of 1 mM ATP.

A double-reciprocal plot of the data in Figure 5 is linear. The derived K_m for ATP is 1 μM, similar to that obtained for

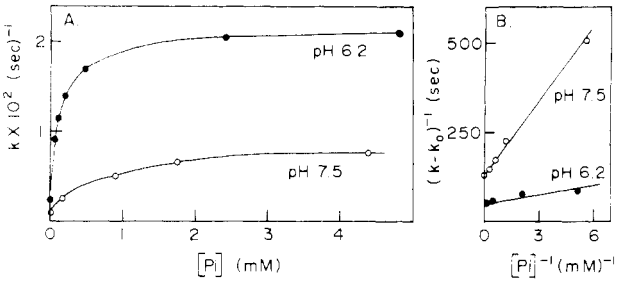

FIGURE 6: Effect of P_i on AO binding rate in rabbit Na,K-ATPase. Conditions were as in Figure 2, curve C, except that the concentration of phosphate was varied as indicated. In (A) the slopes of semilog plots as in Figure 2 are plotted vs. P_i concentration. The rates in the absence of added P_i were 2.3×10^{-3} and 7.5×10^{-4} s^{-1} at pH 6.2 and 7.5, respectively. These values were subtracted from the rates in the presence of P_i and plotted in double-reciprocal form in (B). The derived maximal rates are 1.9×10^{-2} s^{-1} at pH 6.2 and 7.4×10^{-3} s^{-1} at pH 7.5. The apparent K_m values are given in the text.

Na-ATPase activity in the same enzyme preparations.

In Chelex-treated solutions, AO binding was not observed in the presence of P_i alone. However, in the presence of ATP alone or ATP + Na, high concentrations of CDTA were necessary to prevent AO binding. This observation suggests the presence of tightly bound Mg^{2+} in the enzyme and is in agreement with the apparent high affinity of the enzyme for Mg^{2+} in the presence of ATP observed by Skou et al. (1971), Karlish et al. (1978a), and Fukushima & Post (1978).

Effect of P_i. Figure 6A shows the observed pseudo-first-order rate constant of AO binding as a function of P_i concentration for the rabbit enzyme at pH 6.2 and 7.5 in the presence of saturating Mg^{2+}. All Na,K-ATPase preparations we have tested exhibit a slow rate of AO binding with Mg^{2+} in the absence of added P_i. The Mg^{2+}-dependent binding may be due to low levels of P_i contamination in the enzyme preparations or binding to the nonphosphorylated enzyme. The values for the observed association rate constants in the absence of added P_i at pH 6.2 and 7.5 are both ~0.1 of the maximum rate at saturating P_i. This P_i-independent rate would correspond to the K_4 path of Scheme I. The derived rate constant at a given P_i concentration minus the rate constant k_0 measured in the absence of P_i gives a straight line when its reciprocal is plotted against the reciprocal concentration of P_i (Figure 6B). It can be seen that the increased rate at pH 6.2 vs. pH 7.5 is due to both a decrease in the apparent K_m and an increase in the V_{max}. Similar pH effects have been reported for ouabain binding by Yoda & Yoda (1978). The apparent K_m for the promotion of AO binding by P_i in the presence of Mg^{2+} is 0.13 and 0.57 mM at pH 6.2 and 7.5, respectively, for the rabbit enzyme. The concentrations of phosphate monoanion and phosphate dianion at pH 6.2 and 7.5 when the total P_i concentration equals the above K_m values can be estimated by using $pK_a = 6.8$ for P_i at the ionic strength of these assays. For the rabbit enzyme the concentration of monoanion when $[P_i]_{total} = K_m$ is ~0.1 mM at both pH 6.2 and 7.5, while the concentration of dianion varies from 0.02 mM at pH 6.2 to 0.48 mM at pH 7.5. Thus, the increase in apparent K_m for P_i with increasing pH appears to be correlated with the change in phosphate monoanion concentration with pH, which suggests that the monoanion is the more effective P_i species for promotion of AO binding. However, since V_{max} is 2.6 times higher at pH 6.2 than at pH 7.5, dissociable groups on the enzyme may be implicated in these pH effects. These conclusions were also reached by Yoda & Yoda (1978) for ouabain binding.

Effect of Divalent Cations. Figure 7 shows the initial rate of AO binding to eel and rabbit Na,K-ATPase at pH 6.2 as

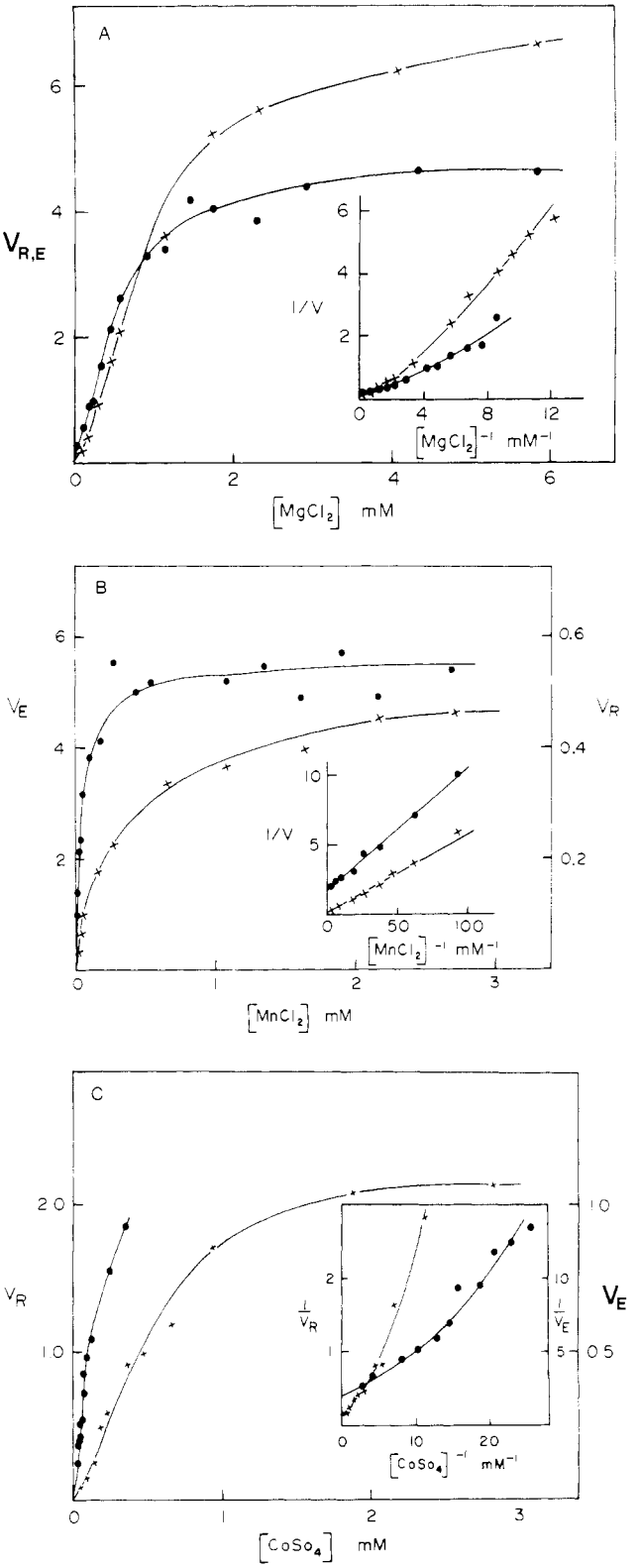

FIGURE 7: Effect of Mg, Mn, and Co on the initial rate of AO binding in the presence of P_i. The initial rates, V_E and V_R, for the eel (×) and rabbit enzymes (●), respectively, are expressed in arbitrary fluorescence units per time divided by the enzyme concentration, and separate scales for V_E and V_R are used as indicated in (B) and (C). The rates obtained in the presence of Co^{2+} were corrected for quenching as described under Materials and Methods. The binding reactions were carried out in the presence of 45 mM Pipes–Tris (pH 6.2), 2.7 μM AO, 3 mM P_i, and 19.3 μg/mL rabbit ATPase or 25 μg/mL eel ATPase, except for the Co^{2+} titration with the eel enzyme which was carried out in 94 mM Pipes–Tris and the Mg titrations with the eel enzyme which had 10 mM P_i. Also the Mg titration with the rabbit enzyme was carried out at 28 °C instead of 25 °C.

Table II: Kinetic Parameters of Divalent Cations for the Rate of P_i-Promoted AO Binding to the Na,K-ATPase[a]

	rabbit		eel	
cation	$K_{0.5}$ (mM)	n	$K_{0.5}$ (mM)	n
Mn^{2+}	0.05	1.01	0.36	0.98
Co^{2+}	0.16	1.31	0.61	1.39[b]
Mg^{2+}	0.57	1.44[c]	1.1	1.34
Mg^{2+}	0.35	1.58[d]	1.2	1.37[e]
Mg^{2+}			0.98	1.53[f]
Mg^{2+}			0.32	1.50[g]

[a] $K_{0.5}$ and n were derived from Hill plots of data as in the experiments shown in Figure 7. Experimental conditions: 45 mM Pipes-Tris (pH 6.2), 2.7 μM AO, 3 mM phosphate-Tris, 19.3 μg/mL eel Na,K-ATPase, 25 °C, except where indicated. Divalent cation concentrations were varied in the ranges shown in Figure 7. Footnotes *e-g* denote the kinetic parameters for Mg^{2+} in the eel enzyme for experiments where the pH or the AO, phosphate, or enzyme concentrations were different. [b] 94 mM Pipes-Tris, pH 6.2. [c] Temperature was 28 °C instead of 25 °C. [d] 32 μg/mL rabbit Na,K-ATPase, 3.3 μM AO, and 4.8 mM phosphate-Tris. [e] Reaction was pseudo first order in enzyme, as in curve D of Figure 2: 0.23 mg/mL eel Na,K-ATPase, 0.038 μM AO, 5 mM phosphate-Tris. [f] 10 mM phosphate-Tris. [g] 12 mM phosphate-Tris and 47 mM Hepes-Tris, pH 7.5.

a function of Mg^{2+}, Mn^{2+}, or Co^{2+} concentration in the presence of P_i. In contrast with ATP and P_i, the rate vs. concentration plots with Mg^{2+} and Co^{2+} are sigmoid, giving nonlinear double-reciprocal plots that curve upward (parts A and C of Figure 7), in both the rabbit and eel Na,K-ATPases. On the other hand, the plots for Mn^{2+} appear hyperbolic and give linear double-reciprocal plots in both enzymes (Figure 7B). Similar sigmoid curves were obtained by plotting the apparent association rate constant derived from the slope of semilog plots as in Figure 2 for the rabbit enzyme. Thus, the sigmoid rate vs. concentration curves are not due to errors in drawing a tangent to the initial region of the fluorescence trace. Hill plots of the experiments in Figure 6 gave Hill coefficients, n, of 1.0 for Mn^{2+} and 1.3–1.5 for Mg^{2+} and Co^{2+} in both enzymes (Table II). If the affinities for divalent cations are compared by the half-maximal concentrations for the binding velocity ($K_{0.5}$ in Table II), the affinities follow their sequence of decreasing ionic radius: $Mn^{2+} > Co^{2+} > Mg^{2+}$ for both eel and rabbit enzymes. Rossi et al. (1978) obtained the same sequence for activation of K^+-phosphatase activity in crab nerve Na,K-ATPase, and we have also observed the same sequence for K^+-phosphatase activity in the eel and rabbit enzymes. The rabbit enzyme has a lower $K_{0.5}$ for activation of AO binding than the eel enzyme for all the cations. The V_{max} values estimated from the data in Figure 7 cannot be directly compared since the initial rate is measured as relative fluorescence units per minute. A comparison of the apparent half-time of binding under the same conditions with Mn^{2+}, Mg^{2+}, and Co^{2+} indicated that the maximal AO binding rates are similar, except for the rabbit enzyme with Mn^{2+} where the maximal rate is about a fifth of that with Mg^{2+}, as noted in Figure 1. Since k_{off} is the same with Mn^{2+}, the slower k_{on} indicates that the affinity for AO is lower with this cation. This is consistent with the lower fluorescence at equilibrium (Figure 1C), suggesting that less AO is bound.

At pH 7.5 the $K_{0.5}$ for Mg^{2+} in the eel enzyme decreased about threefold without change in the Hill coefficient (Table II). Increasing the concentration of P_i also had little effect on the Hill coefficient.

The values of the $K_{0.5}$ and Hill coefficients in Table II were obtained by plotting the rate data vs. the total Mg^{2+} concentrations. Reported values of the stability constants for phosphate complexes of Mn^{2+} and Mg^{2+} range from 80 to 400 M (Smith & Alberty, 1956). If the rate data are plotted as a function of the concentration of either free Mg^{2+} or the MgP_i complex calculated with a stability constant of 300 M, the Hill coefficient is raised or lowered 10% for the MgP_i complex or free Mg^{2+}, respectively, and the $K_{0.5}$ values are ~50% lower than those for total Mg^{2+}. Since we do not know whether the actual ligands are free Mg^{2+}, the MgP_i complex, or both, we have expressed the results in terms of the total divalent cation concentrations.

In these experiments, no attempt was made to maintain the ionic strength constant as the divalent cations concentration was varied. We have observed that the AO binding rate in the presence of Co^{2+} + P_i decreases about fourfold when the buffer concentration is increased from 46 to 94 mM. Since the sigmoid behavior indicates an acceleration of the rate with increasing Mg^{2+} or Co^{2+} concentration, this excludes the possibility that the sigmoid curves are caused by the increased ionic strength due to the divalent cations. Thus, the sigmoid curves in Figure 7 appear to reflect the properties of the enzyme and are not an artifact due to the experimental conditions. This is supported by the differences between Mn^{2+} and Mg^{2+} or Co^{2+} and the $K_{0.5}$ differences between the eel and rabbit enzymes.

Discussion

The available data indicate that AO resembles ouabain in its kinetic parameters and species-specific differences. AO dissociates much faster from the rabbit kidney than from the eel Na,K-ATPase (Table I). In purified pig kidney Na,K-ATPase AO dissociation is even slower than in the eel enzyme since no detectable fluorescence decrease is observed up to 20 min after EDTA or ouabain addition in experiments as in Figures 1 and 4 (E. G. Moczydlowski, unpublished experiments). Quantitatively, the AO dissociation rate at 37 °C and pH 7.5 in the rabbit enzyme with Mg + P_i (2.8×10^{-3} s^{-1}; Fortes, 1977) is comparable to that of ouabain in either rabbit kidney (3.2×10^{-3} s^{-1}) (Schuurmans Stekhoven et al., 1976a) or guinea pig kidney (2.4×10^{-3} s^{-1}) (Erdmann & Schoner, 1973a) under similar ligand conditions. The kidney enzymes of the above species have been shown to have a faster ouabain dissociation rate that results in a lower ouabain affinity (Erdmann & Schoner, 1973a,b; Schuurmans Stekhoven et al., 1976a). To our knowledge ouabain binding rate constants for electric organ have not been published. However, the rate constants for AO in the eel Na,K-ATPase are comparable to those for ouabain and other glycosides measured for the bovine brain enzyme (Yoda & Yoda, 1974a,b, 1977, 1978). At 25 °C and pH 7.3, k_{off} for ouabain is 6.2×10^{-5} and 9.72×10^{-5} s^{-1} for the Mg + P_i and MgATP + Na complexes in bovine brain Na,K-ATPase (Yoda & Yoda, 1974a), while k_{off} for AO in the eel enzyme at pH 6.2 is 8.4×10^{-5} and 1.7×10^{-4} s^{-1}, respectively, for the same complexes and temperatures (Table I). Thus, k_{off} for AO in eel Na,K-ATPase is similar to that of glycosides and at least 50-fold slower than k_{off} of aglycons in brain Na,K-ATPase (Yoda & Yoda, 1974a).

k_{on} for AO binding to the rabbit kidney enzyme at 37 °C (1.5×10^4 M^{-1} s^{-1}; Fortes, 1977) is comparable to $k_{on} = 1.75 \times 10^4$ M^{-1} s^{-1} at 37 °C for ouabain binding to guinea pig kidney enzyme (Erdmann & Schoner, 1973a). k_{on} for AO binding to the eel enzyme at 25 °C is 1.4×10^4 and 1.6×10^4 M^{-1} s^{-1} at pH 6.2 and 7.5, respectively, for the MgATP + Na complex (Table I). These values resemble those for ouabain: $k_{on} = 1.54 \times 10^4$ M^{-1} s^{-1} at saturating Na and pH 7.4 in the bovine brain enzyme (Wallick & Schwartz, 1974) and $k_{on} = 1.06 \times 10^4$ M^{-1} s^{-1} at pH 7.3 (Yoda et al., 1973) at the same temperature. For the Mg + P_i complex the AO association

rate varies between (0.73–2.9) × 10^4 M^{-1} s^{-1} at pH 6.2 and (1.2–6) × 10^3 M^{-1} s^{-1} at pH 7.5. These values compare with 6.11 × 10^3 M^{-1} s^{-1} at pH 7.4 (Wallick & Schwartz, 1974) and 1.33 × 10^4 M^{-1} s^{-1} at pH 7.3 (Yoda et al., 1973) in bovine brain for ouabain at the same temperature. The similarity in the kinetic parameters of AO and ouabain indicates that AO is a powerful tool for spectroscopic studies of cardiac glycoside receptors.

AO binding follows pseudo-first-order kinetics in the rabbit enzyme under all ligand conditions and in the eel enzyme in the presence of MgATP + Na, suggesting that the receptors are kinetically homogeneous. However, pseudo-first-order plots of AO binding to the eel enzyme in the presence of Mg + P_i are nonlinear, regardless of the pH. The nonlinearity in these plots is highly reproducible and fits a sum of two exponentials with similar coefficients under a variety of incubation conditions, such as pH and addition of Na^+, which change the actual rates more than 10-fold without altering the relative proportions of the "fast" and "slow" components. We consider it unlikely that this behavior is due to inactivation of the enzyme during the binding experiment or heterogeneous receptor populations, since the AO binding capacity is unaltered and Scatchard plots under these conditions are linear, indicating that heterogeneity is only kinetic and not reflected at equilibrium. In contrast, nonlinear Scatchard plots of [^{3}H]-ouabain binding have been associated with enzyme inactivation in rat skeletal muscle Na,K-ATPase (Erdmann et al., 1976) and in brain Na,K-ATPase (Taniguchi & Iida, 1972; Hansen, 1976) with heterogeneous receptor populations (Sweadner, 1979). When the concentration of eel enzyme is in large excess over that of AO, we observe simple first-order binding kinetics (Figure 2, curve D). This is to be expected if the "fast" binding sites are selected under these conditions. Thus, it is possible that the observed AO binding kinetics with Mg + P_i in the eel Na,K-ATPase reflect the existence of two or more conformations that bind AO at different rates and interconvert slowly compared to the rate of AO binding. We do not think that the linearization of the AO kinetic binding plots by low K^+ concentrations (Figure 3) is related to the linearization of Scatchard plots of [^{3}H]ouabain binding to a brain enzyme by K^+ (Hansen, 1976), since the latter preparation has been shown to contain two different Na,K-ATPases with different ouabain affinity (Sweadner, 1979).

The dependence of AO binding kinetics on ligand concentration was analyzed by using the simple model in Scheme I and the assumption that AO binding is slower than ligand binding and/or phosphorylation. This appears adequate for ATP and P_i, since they exhibit Michaelis–Menten kinetics with K_m values similar to those reported for phosphorylation, Na,K-ATPase activity, and P_i–H_2O exchange (Froelich et al., 1976; Mårdh & Zetterqvist, 1974; Robinson, 1976; Dahms & Boyer, 1973).

On the other hand, Mg^{2+} and Co^{2+} exhibit sigmoid velocity vs. concentration plots. However, with the exception of a report that the $K_{0.5}$ for K^+ activation of the K^+-phosphatase activity increases sigmoidally with Mg^{2+} concentration (Swann & Albers, 1978), several studies of the dependence of partial reactions of the Na,K-ATPase on Mg^{2+} concentration have reported simple hyperbolic behavior, including the initial rate of K^+-phosphatase activity and the equilibrium level of phosphorylation by P_i (Gache et al., 1976; Swann & Albers, 1978; Kuriki et al., 1976), the enthalpy change for Mg^{2+} binding (Kuriki et al., 1976), the k_{on} for digoxigenin and ouabain binding (Yoda et al., 1973; Yoda & Yoda, 1977), and the K_D for ouabain (Hansen & Skou, 1973). Thus, it is not clear that the sigmoid behavior in Figure 7 is a general phenomenon applicable to other cardiac glycosides that would suggest cooperative effects in the Na,K-ATPase.

A possible explanation for the sigmoid behavior is that enzyme phosphorylation, rather than AO binding, is rate limiting at low Mg^{2+} or Co^{2+} concentrations. Kuriki et al. (1976) have shown that in the eel enzyme the rate of phosphorylation by P_i has a half-time of ~30 s at 24 °C, pH 6, in the absence of K^+ and in the presence of 5 mM $MgCl_2$, conditions similar to those used in some of our experiments. The rate-limiting step could change from phosphorylation to the actual AO binding step as the divalent cation concentration is increased, causing the sigmoidicity. Other possible explanations include more complicated kinetic models than Scheme I, nonspecific binding of divalent cations to phospholipids, or more than one Mg^{2+} site on the enzyme. The available data do not permit us to distinguish between these possibilities.

Regardless of which of the above interpretations is correct, Mn^{2+} behaves differently in both enzymes, giving linear double-reciprocal plots of AO binding rate vs. Mn^{2+} concentration. In addition, the maximal AO binding rate with Mn^{2+} is ~5 times slower than that with Mg^{2+} or Co^{2+} in the rabbit but not the eel Na,K-ATPase. The reasons for the different behavior of Mn^{2+} are not clear. Binding of Mn^{2+} to sheep kidney Na,K-ATPase measured by magnetic resonance showed a single high-affinity site with a K_D around 1 μM (Grisham & Mildvan, 1974). Our results give a higher $K_{0.5}$ for both AO binding rate and phosphatase activity, which may reflect the species-specific differences in affinity for Mn^{2+} or an overestimation of the binding constant by the kinetic measurements.

It is of interest to compare the information on ligand affinity constants obtained from the kinetic studies with that derived from equilibrium AO binding measurements. Using the kinetic model of Scheme I, it can be shown that the concentration of ligand necessary to give half-maximal AO binding at equilibrium, K_{app}, is given by

$$K_{app} = K_1\left(\frac{1 + [AO]/K_4}{1 + [AO]/K_2}\right) \quad (5)$$

Equation 5 predicts that K_{app} will only equal the true ligand dissociation constant K_1 when the affinity for AO in the presence of the ligand (K_2) equals the AO affinity in the absence of the ligand (K_4).

Since it is evident that all the ligands that promote AO binding also increase the affinity of the receptor (i.e., decrease the AO dissociation constant K_2), then $K_2 \ll K_4$ in the presence of the ligand. In the limit, when AO does not bind in the absence of a ligand, $K_4 \simeq \infty$ and eq 5 reduces to

$$K_{app} = \frac{K_1}{1 + [AO]/K_2} \quad (6)$$

Thus, K_{app} will be significantly smaller than the true ligand dissociation constant K_1 when measurements are done with AO concentrations equal to or higher than its dissociation constant, K_2. Under our conditions, [AO] = 3 × 10^{-6} M and K_2 = 10^{-8}–10^{-7} M, so that K_{app} should be 1 to 2 orders of magnitude smaller than K_1. That this is the case is shown by the observation that AO binding at equilibrium (measured as ΔF_∞) was more than half-saturated even at the lowest Mg^{2+} concentration tested (78 μM), in contrast with the kinetic measurements where the half-maximal rate of AO binding was with 0.35 mM Mg^{2+}. A similar difference between the concentrations necessary for half-maximal rate or equilibrium AO

binding was observed with Mn^{2+}, Co^{2+}, P_i, and ATP.

Acknowledgments

We thank Adrianne Farkas for excellent technical assistance and Kathleen Walsh and Laura Bass for preparing the manuscript.

References

Albers, R. W., Koval, G. J., & Siegel, G. J. (1968) *Mol. Pharmacol. 4*, 324.
Choi, Y. R., & Akera, T. (1977) *Biochim. Biophys. Acta 481*, 648.
Choi, Y. R., & Akera, T. (1978) *Biochim. Biophys. Acta 508*, 313.
Dahms, A. S., & Boyer, P. D. (1973) *J. Biol. Chem. 248*, 3155.
Dixon, J. F., & Hokin, L. E. (1974) *Arch. Biochem. Biophys. 163*, 749.
Erdmann, E., & Schoner, W. (1973a) *Biochim. Biophys. Acta 307*, 386.
Erdmann, E., & Schoner, W. (1973b) *Biochim. Biophys. Acta 330*, 302.
Erdmann, E., Phillip, G., & Tanner, G. (1976) *Biochim. Biophys. Acta 455*, 287.
Fortes, P. A. G. (1977) *Biochemistry 16*, 531.
Fortes, P. A. G., & Moczydlowski, E. G. (1977) *J. Gen. Physiol. 70*, 7a.
Froelich, J. P., Albers, R. W., Koval, G. J., Goebel, R., & Berman, M. (1976) *J. Biol. Chem. 251*, 2186.
Fukushima, Y., & Post, R. L. (1978) *J. Biol. Chem. 253*, 6583.
Gache, C., Rossi, B., & Lazdunski, M. (1976) *Eur. J. Biochem. 65*, 293.
Gache, C., Rossi, B., & Lazdunski, M. (1977) *Biochemistry 16*, 2957.
Glynn, I. M. (1964) *Pharmacol. Rev. 16*, 381.
Good, N. E., Winget, G. D., Winter, W., Connolly, T. N., Izaua, S., & Singh, R. M. M. (1966) *Biochemistry 5*, 467.
Grisham, C. M., & Mildvan, A. S. (1974) *J. Biol. Chem. 249*, 3187.
Hansen, O. (1976) *Biochim. Biophys. Acta 433*, 383.
Hansen, O., & Skou, J. C. (1973) *Biochim. Biophys. Acta 311*, 51.
Jesaitis, A. J., & Fortes, P. A. G. (1980) *J. Biol. Chem.* (in press).
Jorgensen, P. L. (1974a) *Biochim. Biophys. Acta 356*, 36.
Jorgensen, P. L. (1974b) *Biochim. Biophys. Acta 356*, 53.
Karlish, S. J. D., Yates, D. W., & Glynn, I. M. (1978a) *Biochim. Biophys. Acta 525*, 230.
Karlish, S. J. D., Yates, D. W., & Glynn, I. M. (1978b) *Biochim. Biophys. Acta 525*, 252.
Kuriki, Y., Halsey, J., Biltonen, R., & Racker, E. (1976) *Biochemistry 15*, 4956.
Kyte, J. (1972) *J. Biol. Chem. 247*, 7634.
Mårdh, D., & Zetterqvist, O. (1974) *Biochim. Biophys. Acta 350*, 473.
Moczydlowski, E. G., & Fortes, P. A. G. (1977a) *Biophys. J. 17*, 225a.
Moczydlowski, E. G., & Fortes, P. A. G. (1977b) *J. Supramol. Struct., Suppl. 1*, 153.
Perrone, J. R., Hackney, J. F., Dixon, J. F., & Hokin, L. E. (1975) *J. Biol. Chem. 250*, 4178.
Post, R. L. (1977) *FEBS Symp. No. 42*, 352.
Post, R. L., Toda, G., & Rogers, F. N. (1975) *J. Biol. Chem. 250*, 691.
Robinson, J. D. (1976) *Biochim. Biophys. Acta 429*, 1006.
Rossi, B., Gache, C., & Lazdunski, M. (1978) *Eur. J. Biochem. 85*, 561.
Schuurmans Stekhoven, F. M. A. H., De Pont, J. J. H. H. M., & Bonting, S. L. (1976a) *Biochim. Biophys. Acta 419*, 137.
Schuurmans Stekhoven, F. M. A. H., van Heeswijk, M. P. E., De Pont, J. J. H. H. M., & Bonting, S. L. (1976b) *Biochim. Biophys. Acta 422*, 210.
Schwartz, A., Matsui, H., & Laughter, A. H. (1968) *Science 160*, 323.
Schwartz, A., Lindenmayer, G. E., & Allen, J. C. (1975) *Pharmacol. Rev. 27*, 3.
Sen, A. K., Tobin, T., & Post, R. L. (1969) *J. Biol. Chem. 244*, 6596.
Skou, J. C., Butler, K. W., & Hansen, O. (1971) *Biochim. Biophys. Acta 241*, 443.
Smith, R. M., & Alberty, R. A. (1956) *J. Am. Chem. Soc. 78*, 2376.
Swann, A. C., & Albers, R. W. (1978) *Biochim. Biophys. Acta 523*, 215.
Sweadner, K. (1979) *J. Biol. Chem. 254*, 6060.
Taniguchi, K., & Iida, S. (1972) *Biochim. Biophys. Acta 288*, 98.
Taussky, H., & Schorr, E. (1953) *J. Biol. Chem. 202*, 675.
Wallick, E. T., & Schwartz, A. (1974) *J. Biol. Chem. 249*, 5141.
Willard, J. M., Davis, J. J., & Wood, H. G. (1969) *Biochemistry 8*, 3137.
Yoda, A. (1974) *Ann. N.Y. Acad. Sci. 242*, 598.
Yoda, A., & Yoda, S. (1974a) *Mol. Pharmacol. 10*, 494.
Yoda, A., & Yoda, S. (1974b) *Mol. Pharmacol. 10*, 810.
Yoda, A., & Yoda, S. (1977) *Mol. Pharmacol. 13*, 352.
Yoda, A., & Yoda, S. (1978) *Mol. Pharmacol. 14*, 624.
Yoda, A., Yoda, S., & Sarrif, A. M. (1973) *Mol. Pharmacol. 9*, 766.